Available online at www.sciencedirect.com
ScienceDirect
International Journal of Rock Mechanics & Mining Sciences 45 (2008) 1226–1236
International Journal of Rock Mechanics and Mining Sciences
www.elsevier.com/locate/ijrmms

How sorption-induced matrix deformation affects gas flow in coal seams: A new FE model

Hongbin Zhang[a,c], Jishan Liu[a,*], D. Elsworth[b]

[a]School of Oil and Gas Engineering, The University of Western Australia, WA 6009, Australia
[b]Department of Energy and Geo-Environmental Engineering, Penn State University, USA
[c]Hainan University, Hainan Province, PR China

Received 21 December 2006; received in revised form 28 November 2007; accepted 30 November 2007
Available online 15 January 2008

Abstract

The influence of sorption-induced coal matrix deformation on the evolution of porosity and permeability of fractured coal seams is evaluated, together with its influence on gas recovery rates. The porosity-based model considers factors such as the volume occupied by the free-phase gas, the volume occupied by the adsorbed phase gas, the deformation-induced pore volume change, and the sorption-induced coal pore volume change. More importantly, these factors are quantified under in situ stress conditions. A cubic relation between coal porosity and permeability is introduced to relate the coal storage capability (changing porosity) to the coal transport property (changing permeability). A general porosity and permeability model is then implemented into a coupled gas flow and coal deformation finite element model. The new FE model was used to compare the performance of the new model with that of the Palmer–Mansoori model. It is found that the Palmer–Mansoori model may produce significant errors if loading conditions deviate from the assumptions of the uniaxial strain condition and infinite bulk modulus of the grains. The FE model was also applied to quantify the net change in permeability, the gas flow, and the resultant deformation in a coal seam. Model results demonstrate that the evolution of porosity and of permeability is controlled by the competing influences of effective stresses and sorption-based volume changes. The resulting sense of permeability change is controlled by the dominant mechanism.

Keywords: Matrix shrinking; Coal permeability; Coal porosity; Coupled model; Simulation

1. Introduction

Methane in coal seams is an important natural energy resource, although ignition and the resulting explosion hazard remain a major problem during coal mining. Degassing seams is an important method to mitigate this hazard, and results in the beneficial recovery of a clean-burning and low-carbon fuel resource. The injection of carbon dioxide to preferentially dissociate methane has been an effective measure used after primary recovery by depressurization. Recently, carbon dioxide (CO_2) sequestration in deep coal seams has attracted more attention as a method of reducing the output of greenhouse gases to the atmosphere [1].

Gas flow within coal seams is quite different from that of conventional reservoirs. Detailed studies have examined the storage and transport mechanisms of gas in coal seams. In situ and laboratory data indicate that the storage and flow of gas in coal seams is associated with the matrix structure of coal and the absorption or desorption of gas. Coal is a naturally fractured dual-porosity reservoir [2], consisting of micro-porous matrix and cleats. Most of the gas is initially stored within micro-pores in the absorbed state [3]. When gas recovery begins, the gas desorbs and diffuses from matrix to cleats due to the concentration gradient. The gas flowing through the cleats is considered to be gas seepage controlled by the permeability of the coal seam [4]. Experimental results have shown that gas sorption generally follows a Langmuir isotherm [5,6]. Desorption plays an important role in both defining the longevity and rate of the gas supply, and in controlling the

*Corresponding author. Tel.: +61 8 6488 7205; fax: +61 8 6488 1964.
E-mail address: Jishan@cyllene.uwa.edu.au (J. Liu).

1365-1609/$ - see front matter © 2008 Elsevier Ltd. All rights reserved.
doi:10.1016/j.ijrmms.2007.11.007

related deformation of the solid matter comprising the seam.

A variety of experiments have investigated sorption characteristics under isothermal conditions [4,7–10] with supporting models representing isothermal response [8,9,11–13]. These studies have also noted the dependency of volumetric strain of the coal matrix as a non-linear function of gas pressure, driven by gas desorption. There is an approximately linear relationship between the sorption-induced volumetric strain and the absorbed gas volume [7,9,10]. This relation holds both during uptake, described as sorption, and in discharge, described as desorption, of gases from the surfaces of the coal matrix. Because of the dual-porosity structure of coal seams (i.e., micro-porous matrix and macro-porous cleat/fracture network), the coal matrix represents the main reservoir for the gas, and the cleats the main fracture pathways. When the pore pressure declines during methane production, methane desorbs from the coal matrix and the desorbed gas flows through the cleats to the producing well. The decline of pore pressure results in a concomitant increase in effective stress. The increase in effective stress reduces the stress-sensitive permeability of the cleat system. In contrast, the desorption-induced shrinkage of the coal matrix widens the cleats and enhances permeability. The net change in permeability accompanying gas production is thus controlled by the competitive effects of declining pore pressure decreasing permeability, and the shrinking coal matrix increasing permeability. The net effect, of permeability loss or permeability gain, is dependent on the mechanical boundary conditions applied to the system.

Adsorption of gas, such as carbon dioxide, is the reverse of desorption. When the gas pressure increases, the gas adsorbs onto the coal matrix. The increase of pore pressure results in a decrease of effective stress. The reduction in effective stress enhances the coal permeability. In contrast, the adsorption-induced swelling of the coal matrix reduces the cleat apertures and decreases the permeability. The net change in permeability accompanying gas sequestration is also controlled competitively by the influence of effective stresses and matrix swelling, again controlled by the boundary conditions applied locally between the end-members of null changes in either mean stress or volume strain.

Numerical simulations of gas diffusion, gas flow, and coupled hydromechanical response have been widely applied. Finite element methods and a formulation for modeling mass transport problems in porous media have been applied, including the effects of coupled solid–gas response for gas flow in coal seams [14]. This included only the effect of gas sorption on mass storage [15]. Valliappan and Zhang developed a coupled model incorporating the effect of diffusion of adsorbed methane gas from the solid matrix to the voids [16]. A dual-porosity poroelastic model was extended and utilized in solving generalized plane strain problems [17,18]. Gilman and Beckie proposed a simplified model of methane diffusion and transport in a coal seam and found a reference time of methane release from the coal matrix into cleats to have a critical influence on overall methane production [19]. A model for multi-phase flow, coupled with heat transfer and rock deformation, was used to simulate CO_2 injection into a brine formation by Rutqvist and Tsang [20]. In 2004, a non-linear coupled mathematical model of solid deformation and gas seepage was presented and the methane extraction from fractured coal seam was simulated [21]. However, the constitutive relationships between stress and strain are similar to conventional poroelastic mechanics in most of the above simulations and the effect of sorption-induced strain on matrix volumetric strain has not been taken into account although experimental data have noted its significant impact—both on total volumetric strain of the seam, and the resulting feedback on permeability.

The gas flow in coal seams is a complex physical and chemical process coupling solid deformation, gas desorption and gas movement. Although the influence of sorption-induced deformation on porosity, and on permeability has been widely studied, how this in turn affects gas flow within the seam is not well understood. This is partly because no coupled gas flow and sorption-induced coal deformation models are available for in situ stress conditions. The primary motivation of this study is to investigate how sorption-induced coal matrix deformation affects the gas flow in a coal seam through developing such a porosity-based model.

2. Governing equations

In the following, a set of field equations are defined which govern the deformation of the solid matrix, and prescribe the transport and interaction of gas flow in a similar way to poroelastic theory [22]. These derivations are based on the following assumptions: (a) coal is a homogeneous, isotropic and elastic continuum. (b) Strains are much smaller than the length scale. (c) Gas contained within the pores is ideal, and its viscosity is constant under isothermal conditions. (d) The rate of gas flow through the coal is defined by Darcy's law. (e) Conditions are isothermal. (f) Coal is saturated by gas. (g) Compositions of the gas are not competitive, i.e., one gas component at a time.

2.1. Governing equation for coal seam deformation

For a homogeneous, isotropic and elastic medium, the strain-displacement relation is expressed as

$$\varepsilon_{ij} = \tfrac{1}{2}(u_{i,j} + u_{j,i}), \tag{1}$$

where ε_{ij} is the component of the total strain tensor and u_i is the component of the displacement. The equilibrium equation is defined as

$$\sigma_{ij,j} + f_i = 0, \tag{2}$$

where σ_{ij} denotes the component of the total stress tensor and f_i denotes the component of the body force. The

following conventions have been adopted in Eqs. (1) and (2) and following related equations: a comma followed by subscripts denotes differentiation with respect to spatial coordinates and repeated indices in the same monomial imply summation over the range of the indices (generally 1–3, unless otherwise indicated) [23].

The gas sorption-induced strain ε_s is presumed to result in volumetric strain only. Its effects on all three normal components of strain are same. On the basis of poroelasticity [23] and by making an analogy between thermal contraction and matrix shrinkage [12], the constitutive relation for the deformed coal seam becomes

$$\varepsilon_{ij} = \frac{1}{2G}\sigma_{ij} - \left(\frac{1}{6G} - \frac{1}{9K}\right)\sigma_{kk}\delta_{ij} + \frac{\alpha}{3K}p\delta_{ij} + \frac{\varepsilon_s}{3}\delta_{ij}, \tag{3}$$

where $G = E/2(1+\nu)$, $K = E/3(1-2\nu)$, $\alpha = 1-K/K_s$, and $\sigma_{kk} = \sigma_{11}+\sigma_{22}+\sigma_{33}$, where K is the bulk modulus of coal, K_s is the bulk modulus of the coal grains, G is the shear modulus of coal, E is the Young's modulus of coal, ν is Possion's ratio of coal, α is the Biot coefficient, δ_{ij} is the Kronecker delta, and p is the gas pressure within the pores. From Eq. (3), we obtain

$$\varepsilon_v = -\frac{1}{K}(\bar{\sigma} - \alpha p) + \varepsilon_s, \tag{4}$$

where $\varepsilon_v = \varepsilon_{11}+\varepsilon_{22}+\varepsilon_{33}$ is the volumetric strain of coal matrix and $\bar{\sigma} = -\sigma_{kk}/3$ is the mean compressive stress. The component of effective stress σ_{eij} is also defined as $\sigma_{eij} = \sigma_{ij}+\alpha p\delta_{ij}$. Combination of Eqs. (1)–(3) yields the Navier-type equation expressed as

$$Gu_{i,kk} + \frac{G}{1-2\nu}u_{k,ki} - \alpha p_{,i} - K\varepsilon_{s,i} + f_i = 0. \tag{5}$$

Eq. (5) is the governing equation for coal deformation, where the gas pressure, p, can be solved from the gas flow equation as discussed following.

2.2. Governing equation for gas flow

The equation for mass balance of the gas is defined as

$$\frac{\partial m}{\partial t} + \nabla\cdot(\rho_g \boldsymbol{q}_g) = Q_s, \tag{6}$$

where ρ_g is the gas density, $\boldsymbol{q}_g$ is the Darcy velocity vector, Q_s is the gas source or sink, t is the time, and m is the gas content including free-phase gas and absorbed gas [1], is defined as

$$m = \rho_g\phi + \rho_{ga}\rho_c\frac{V_L p}{p+P_L}, \tag{7}$$

where ρ_{ga} is the gas density at standard conditions, ρ_c is the coal density, ϕ is porosity, V_L represents the Langmuir volume constant, and P_L represents the Langmuir pressure constant. According to the ideal gas law, the gas density is described as

$$\rho_g = \frac{M_g}{RT}p, \tag{8}$$

where M_g is the molecular mass of the gas, R is the universal gas constant, and T is the absolute gas temperature.

Assuming the effect of gravity is relatively small and can be neglected, the Darcy velocity, $\boldsymbol{q}_g$, is given by

$$\boldsymbol{q}_g = -\frac{k}{\mu}\nabla p, \tag{9}$$

where k is the three permeability of the coal and μ is the dynamic viscosity of the gas. Substituting Eqs. (7)–(9) into Eq. (6), we obtain

$$\left[\phi + \frac{\rho_c p_a V_L P_L}{(p+P_L)^2}\right]\frac{\partial p}{\partial t} + p\frac{\partial\phi}{\partial t} - \nabla\cdot\left(\frac{k}{\mu}p\nabla p\right) = Q_s, \tag{10}$$

where p_a is one atmosphere of pressure (101.325 kPa). In Eq. (10), the permeability k is dependent on the porosity, ϕ, while ϕ is a function of the volumetric strain, ε_v, and the sorption-induced strain, ε_s. Therefore, Eqs. (5) and (10) are coupled through the porosity–permeability relation.

2.3. A general porosity model

The sorption-induced volumetric strain ε_s is fitted onto Langmuir-type curves and has been verified through experiments [7,9,10]. A Langmuir-type equation is used to calculate this volumetric strain, defined as

$$\varepsilon_s = \varepsilon_L\frac{p}{P_L+p}, \tag{11}$$

where the Langmuir volumetric strain, ε_L, is a constant representing the volumetric strain at infinite pore pressure and the Langmuir pressure constant, P_L, representing the pore pressure at which the measured volumetric strain is equal to $0.5\varepsilon_L$. The authors in the above experiments also assume that the coal permeability varies with porosity as follows:

$$\frac{k}{k_0} = \left(\frac{\phi}{\phi_0}\right)^3, \tag{12}$$

where the subscript, 0, denotes the initial value of the variable. The porosity is calculated as a function of coal mechanical properties such as modulus, sorption isotherm parameters and pore pressure. However, different studies have presented different formulae to calculate the coal porosity and permeability.

2.3.1. Review of porosity and permeability models

In the following, we briefly explain each of the models currently available in the literature, and refer the reader to the source papers for further details.

2.3.1.1. Seidle–Huitt model. This model does not include the elastic strain of the coal and assumes that all permeability changes are caused by the sorption-induced strain only. Under these assumptions, the porosity and

permeability are defined as [2]

$$\frac{\phi}{\phi_0} = 1 + \frac{\varepsilon_L}{3}\left(1 + \frac{2}{\phi_0}\right)\left(\frac{p_0}{P_L + p_0} - \frac{p}{P_L + p}\right), \tag{13}$$

$$\frac{k}{k_0} = \left[1 + \frac{\varepsilon_L}{3}\left(1 + \frac{2}{\phi_0}\right)\left(\frac{p_0}{p_L + p_0} - \frac{p}{p_L + p}\right)\right]^3. \tag{14}$$

2.3.1.2. Palmer–Mansoori model. Unlike the Seidle–Huitt model, the Palmer–Mansoori model considers the elastic deformation of coal under uniaxial stress conditions. The porosity model is defined as [11]

$$\frac{\phi}{\phi_0} = 1 + \frac{1}{M\phi_0}(p - p_0) + \frac{\varepsilon_L}{3\phi_0}\left(\frac{K}{M} - 1\right)\left(\frac{p}{P_L + p} - \frac{p_0}{P_L + p_0}\right), \tag{15}$$

$$\frac{k}{k_0} = \left[1 - \frac{1}{M\phi_0}(p - p_0) + \frac{\varepsilon_L}{\phi_0}\left(\frac{K}{M} - 1\right)\left(\frac{p}{P_L + p} - \frac{p_0}{P_L + p_0}\right)\right]^3, \tag{16}$$

where $M = E(1-v)/(1+v)(1-2v)$.

2.3.1.3. Shi–Durucan model. The assumptions are same as the Palmer–Mansoori model [12]:

$$\frac{k}{k_0} = \exp\left\{3c_f\left[\frac{v}{1-v}(p - p_0) + \frac{\varepsilon_L}{3}\left(\frac{E}{1-v}\right) \times \left(\frac{p_0}{P_L + p_0} - \frac{p}{P_L + p}\right)\right]\right\}, \tag{17}$$

where c_f is cleat volume compressibility.

2.3.1.4. Cui–Bustin model. This model has a general form but it is only applied to the same assumed situation as the Palmer–Mansoori model [9]:

$$\frac{\phi}{\phi_0} = \exp\left\{\left(\frac{1}{K} - \frac{1}{K_p}\right)[(\sigma - \sigma_0) - (p - p_0)]\right\}, \tag{18}$$

$$\frac{k}{k_0} = \exp\left\{-\frac{3}{K_p}[(\sigma - \sigma_0) - (p - p_0)]\right\}, \tag{19}$$

where K_p is the bulk modulus of pores.

2.3.1.5. Robertson–Christiansen model. In this model, the deformation of coal grains is neglected and equal axial and radial stresses are assumed [13].

$$\frac{k}{k_0} = \exp\left\{-3c_0\frac{1 - \exp[\alpha_c(p - p_0)]}{\alpha} + \frac{9}{\phi_0}\left[\frac{1-2v}{E}(p - p_0) - \frac{\varepsilon_L}{3}\left(\frac{P_L}{P_L + p_0}\right)\mathrm{In}\left(\frac{P_L + p}{P_L + p_0}\right)\right]\right\}, \tag{20}$$

where c_0 is the initial fracture compressibility and α_c is the change rate in fracture compressibility.

In all these models, the total stress, σ, has been assumed as constant, i.e.,

$$d\sigma = d\sigma_e - dp = 0 \quad (\alpha = 1), \tag{21}$$

where σ_e denotes effective stress. Or under invariant total stress.

$$d\sigma_e = dp. \tag{22}$$

According to the principle of effective stress, the induced coal deformation is determined by the change in effective stress, $d\sigma_e$, which can be replaced by the change in pore pressure, dp, under the assumption of null change in total stress. This is why terms representing effective stress or total stress are absent in all of these existing permeability models. However, this condition can be violated in a number of circumstances, including the penetration by drill holes, the massive stimulation by the injection of fluids, and the proximity of excavation surfaces. These factors result in the re-distribution of total stresses in coal seams. Therefore, a new porosity and permeability model under variable stress conditions is needed to quantify the gas flow in coal seams.

2.3.2. The general porosity model

Considering a porous medium containing solid volume of V_s and pore volume of V_p, we assume the bulk volume $V = V_p + V_s$ and the porosity $\phi = V_p/V$. According to Eq. (4), the volumetric evolution of the porous medium with the load of $\bar{\sigma}$ and p can be described in terms of $\Delta V/V$ and $\Delta V_p/V_p$, the volumetric strain of coal and volumetric strain of pore space, respectively [23]. The relations are

$$\frac{\Delta V}{V} = -\frac{1}{K}(\bar{\sigma} - \alpha p) + \varepsilon_s, \tag{23}$$

$$\frac{\Delta V_p}{V_p} = -\frac{1}{K_p}(\bar{\sigma} - \beta p) + \varepsilon_s, \tag{24}$$

where $\beta = 1 - K_p/K_s$.

We assume that the sorption-induced strain for the coal is the same as for the pore space. Without the gas sorption effect, the volumetric variation of the porous medium satisfies the Betti–Maxwell reciprocal theorem [23], $(\partial V/\partial p)_{\bar{\sigma}} = (\partial V_p/\partial\bar{\sigma})_p$, and we obtain

$$K_p = \frac{\phi}{\alpha}K. \tag{25}$$

Using the definition of porosity, the following expressions can be deduced as

$$\frac{\Delta V}{V} = \frac{\Delta V_s}{V_s} + \frac{\Delta\phi}{1-\phi}, \tag{26}$$

$$\frac{\Delta V_p}{V_p} = \frac{\Delta V_s}{V_s} + \frac{\Delta\phi}{\phi(1-\phi)}. \tag{27}$$

Solving Eqs. (23), (24), (26) and (27), we obtain

$$\Delta\phi = \phi\left(\frac{1}{K} - \frac{1}{K_p}\right)(\bar{\sigma} - p). \tag{28}$$

Substituting Eqs. (4) and (25) into Eq. (28) yields

$$\Delta\phi = (\alpha - \phi)\left(\varepsilon_v + \frac{p}{K_s} - \varepsilon_s\right). \tag{29}$$

If the initial porosity is ϕ_0 at pressure p_0 and the initial volumetric strain is zero, the porosity can be expressed as

$$\phi = \frac{1}{1+S}[(1+S_0)\phi_0 + \alpha(S-S_0)], \tag{30}$$

where $S = \varepsilon_v + (p/K_s) - \varepsilon_s$, $S_0 = (p_0/K_s) - \varepsilon_L p_0/(p_0+p_L)$.

Considering the cubic law relation, Eq. (12), between permeability and porosity of the porous media, we obtain

$$\frac{k}{k_0} = \left(\frac{1}{1+S}\left[(1+S_0) + \frac{\alpha}{\phi_0}(S-S_0)\right]\right)^3, \tag{31}$$

where k_0 is the initial permeability at the initial pressure p_0 and porosity ϕ_0.

Eqs. (30) and (31) present a general porosity model and a general permeability model, respectively. These models can be applied to variable stress conditions. If we consider $S \ll 1$ and $S_0 \ll 1$, the simplified expression for porosity is derived as

$$\phi = \phi_0\left\{1 + \frac{\alpha}{\phi_0}\left[\varepsilon_v + \frac{p-p_0}{K_s} + \frac{\varepsilon_L P_L(p_0-p)}{(p_0+P_L)(p+P_L)}\right]\right\}. \tag{32}$$

It is clear that the porosity and permeability of the coal is controlled by the matrix volumetric strain associated with effective stress (Eq. (4)), the grain volumetric strain and the gas desorption-induced volumetric strain. It should be noted that neither matrix volumetric strain nor effective stress is independent of gas desorption-induced strain according to Eq. (4). It is apparent that the general porosity and permeability model is coupled with the coal seam deformation. Both the porosity model and the permeability model define the interactions between coal deformation and gas flow.

If $S \ll 1$, $S_0 \ll 1$, and $K_s \gg K$, the coal seam is under conditions of uniaxial strain, and the overburden load is unchanged, a simplified expression of porosity can be derived from Eq. (30) as

$$\phi = \phi_0 + \frac{(1+v)(1-2v)}{E(1-v)}(p-p_0) - \frac{2(1-2v)}{3(1-v)}\left(\frac{\varepsilon_L p}{p+P_L} - \frac{\varepsilon_L p_0}{p_0+P_L}\right) \tag{33}$$

which is the same as the model presented by Palmer and Mansoori [11]. Using the stress–strain relation and assuming ε_{33} is the direction of uniaxial strain and overburden load, the Palmer–Mansoori model can also be expressed as

$$\phi = \phi_0\left\{1 + \frac{1}{\phi_0}\left[\varepsilon_{33} + \frac{\varepsilon_L P_L(p_0-p)}{(p_0+P_L)(p+P_L)}\right]\right\}. \tag{34}$$

Comparing Eq. (34) with Eq. (32), the Palmer–Mansoori model is only applicable to conditions of uniaxial strain, constant overburden load, and infinite bulk modulus of the grains.

2.4. Coupled governing equations

Substituting Eq. (11) into Eq. (5), we rewrite the governing equation for coal seam deformation as

$$Gu_{i,kk} + \frac{G}{1-2v}u_{k,ki} - \alpha p_{,i} - \frac{K\varepsilon_L P_L}{(p+P_L)^2}p_{,i} + f_i = 0. \tag{35}$$

From Eq. (30), the partial derivative of ϕ with respect to time is expressed as

$$\frac{\partial\phi}{\partial t} = \frac{\alpha-\phi}{1+S}\left[\frac{\partial\varepsilon_v}{\partial t} + \frac{1}{K_s}\frac{\partial p}{\partial t} - \frac{\varepsilon_L P_L}{(p+P_L)^2}\frac{\partial p}{\partial t}\right]. \tag{36}$$

Substituting Eq. (36) into Eq. (10) yields the governing equation for gas flow through a coal seam with gas sorption as

$$\left[\phi + \frac{\rho_c p_a V_L P_L}{(p+P_L)^2} + \frac{(\alpha-\phi)p}{(1+S)K_s} - \frac{(\alpha-\phi)\varepsilon_L P_L p}{(1+S)(p+P_L)^2}\right]\frac{\partial p}{\partial t} - \nabla\cdot\left(\frac{k}{\mu}p\nabla p\right) = Q_s - \frac{(\alpha-\phi)p}{(1+S)}\frac{\partial\varepsilon_v}{\partial t}. \tag{37}$$

The first term on the left-hand side of Eq. (37) represents all the controlling factors on porosity, including the volume occupied by the free-phase gas, the volume occupied by the adsorbed phase gas, the coal mechanical deformation-induced pore volume change, and the sorption-induced coal pore volume change. More importantly, these factors are quantified under in situ stress conditions. The second term on the left-hand side is associated with the characteristics of gas migration. On the right-hand side, the second term is a coupled term including the rate change in the volumetric strain due to coal deformation. Its contribution to the equation can be treated as a source or sink from the mechanical deformation. Therefore, Eqs. (35)–(37) define the coupled gas flow and coal seam deformation model.

2.5. Boundary and initial conditions

For the Navier-type Eq. (35), the displacement and stress conditions on the boundary are given as

$$u_i = \tilde{u}_i(t) \quad \text{on } \partial\Omega, \tag{38}$$

$$\sigma_{ij}n_j = \tilde{F}_i(t) \quad \text{on } \partial\Omega, \tag{39}$$

where $\tilde{u}_i$ and $\tilde{F}_i$ are the known displacements and stresses on the boundary $\partial\Omega$, and n_j is the unit vector normal to the boundary. The initial conditions for displacement and stress in the domain are described as

$$u_i(0) = u_0 \quad \text{in } \Omega, \tag{40}$$

$$\sigma_{ij}(0) = \sigma_0 \quad \text{in } \Omega, \tag{41}$$

where u_0 and σ_0 are initial values of displacement and stress in the domain Ω.

For the gas flow Eq. (37), the Dirichlet and Neumann boundary conditions are defined as

$$p = \tilde{p}(t) \quad \text{on } \partial\Omega, \tag{42}$$

$$\boldsymbol{n}\frac{k}{\mu}\nabla p = \tilde{Q}_s(t) \quad \text{on } \partial\Omega, \tag{43}$$

where $\tilde{p}(t)$ and $\tilde{Q}_s(t)$ are the specified gas pressure and gas flux on the boundary, respectively. The initial condition for gas flow is

$$p(0) = p_0 \quad \text{in } \Omega. \tag{44}$$

3. Finite element implementations

The above governing equations, especially the gas flow equation incorporating the effect of desorption, are a set of non-linear partial differential equations (PDE) of second order in space and first order in time. The non-linearity appears both in the space and time domains; and therefore, these equations are difficult to solve analytically. Therefore, the complete set of coupled equations is implemented into, and solved by using COMSOL Multiphysics, a powerful PDE-based multiphysics modeling environment.

4. Simulation examples

In the following, we present three simulation examples to illustrate the resultant effects of coupled gas sorption and coal deformation. These three examples are under different boundary conditions which causes different stress states. The first one is under uniaxial stress condition. The second one is under constrained plane strain condition. The last one is under unconstrained plane strain condition. We use the three examples to quantify the net change in permeability, in gas flow, and in coal deformation accompanying gas production. These processes are controlled competitively by increases in effective stresses and matrix shrinkage. The results are also compared with Palmer–Mansoori model, respectively, to show the limitation of assumptions in Palmer–Mansoori model.

4.1. Example I: gas desorption under uniaxial stress conditions

In this example, we follow methane desorption from a coal sample under conditions of uniaxial strain. This geometry represents some experimental conditions prescribed in previous published studies and is used to describe the essential characteristics of the gas desorption from coal. The sensitivity of the controlling parameters, including matrix volumetric strain, porosity, permeability and pore pressure, to the gas desorption and the ration of the bulk modulus of coal matrix to that of coal grains (K/K_s) were investigated in detail.

The model geometry of 0.1 m × 0.1 m is shown in Fig. 1. The right side is free to displace while other three sides are constrained. The pressure on the right side is specified as 101.325 kPa. Zero fluxes on the other three sides are specified. The initial gas pore pressure in the coal is set at 6.2 MPa. The coal properties are listed in Table 1. Most of the parameters were chosen from the experimental results [10], and unreported parameters were substituted from contemporary literature.

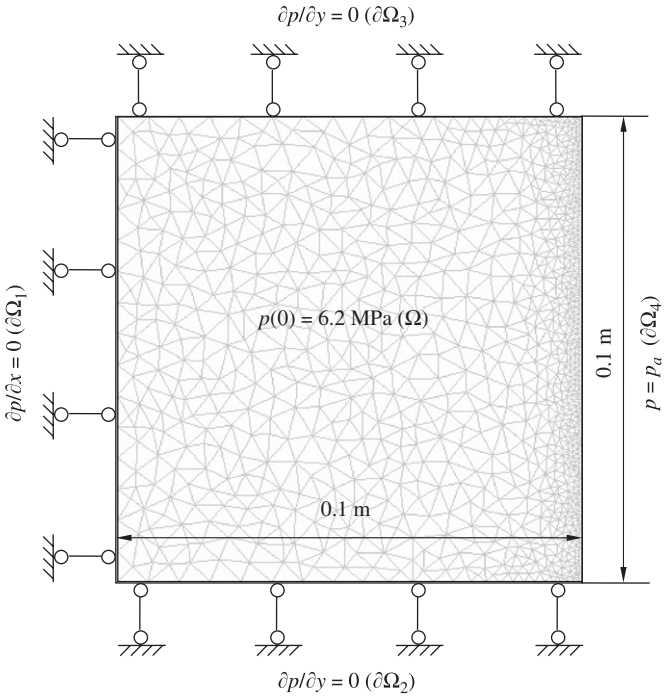

Fig. 1. Example I: simulation model of the gas desorption from a coal sample under the uniaxial plane strain state.

Table 1
Property parameters of Examples I, II, and III

Parameter	Value
Young's modulus of coal, E (MPa)	2713
Young's modulus of coal grains, E_s (MPa)	8139
Possion's ratio of coal, ν	0.339
Density of coal, ρ_c (kg/m^3)	1.25×10^3
Density of methane, ρ_g (kg/m^3) at standard condition	0.717
Methane dynamic viscosity, μ (Pa s)	1.84×10^{-5}
Langmuir pressure constant, P_L (MPa)	6.109
Langmuir volume constant, V_L (m^3/kg)	0.015
Langmuir volumetric strain constant, ε_L	0.02295
Initial porosity of coal, ϕ_0	0.00804
Initial permeability of coal, k_0 (m^2)	3.7996×10^{-17}

We present the model results in terms of (1) the contributions of different volumetric strains to the total volumetric strain; (2) the contributions of different gas storage terms to the total gas storage capability; (3) the evolution of permeability ratios; (4) the effect of coal bulk modulus ratios on the permeability and the comparison with the PM model; (5) the effect of gas desorption on the gas pressure distribution; (6) the effect of coal bulk modulus ratios on the gas pressure distribution; and (7) the evolution of coal deformation. These results are shown in Figs. 2–8.

4.1.1. Porosity and volumetric strains

As shown in Fig. 2, the porosity varies with the volumetric strains of coal matrix, grains, and gas sorption. When pore pressure declines, the sorption-induced

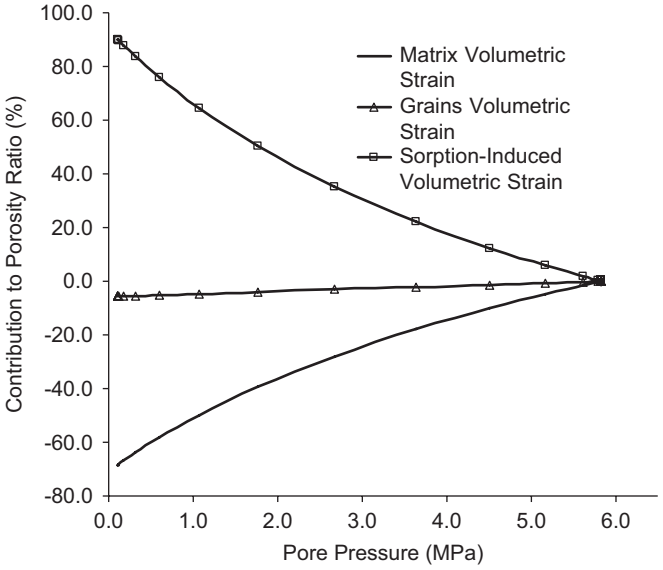

Fig. 2. Example I: contributions of different volumetric strain components to the coal porosity ratio.

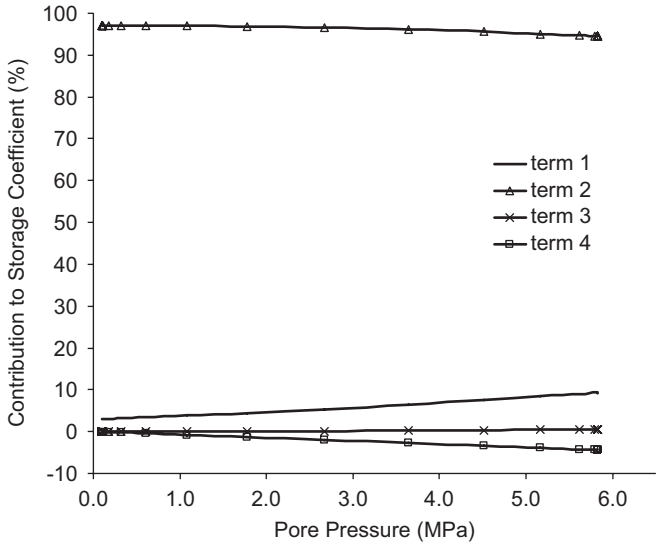

Fig. 3. Example I: contributions of four terms in gas storage coefficient, i.e., the volume occupied by the free-phase gas (term 1), the volume occupied by the adsorbed gas phase (term 2), the mechanical deformation-induced pore volume change (term 3), and the sorption deformation-induced pore volume change (term 4).

volumetric strain is more significant than the bulk mechanical volumetric strain. The contribution from the grain volumetric strain is not obvious.

4.1.2. Gas storage

As shown in Eq. (37), the storage term consists of four contributions: from free gas, from gas absorption, from coal deformation, and from the combined effect of sorption and deformation. Contributions from different sources are presented in Fig. 3. As pore pressure depletes, 94.6–97.1% of the storage coefficient is from gas absorption capability and 9.2–3.0% is from free gas storage capacity. The contributions from the remaining two sources are below 4.5%, and can be neglected.

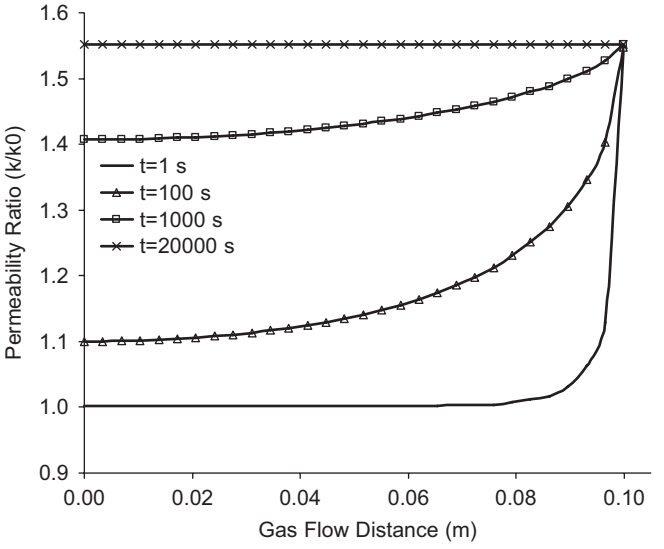

Fig. 4. Example I: spatial and temporal distributions of permeability ratio (k/k_0).

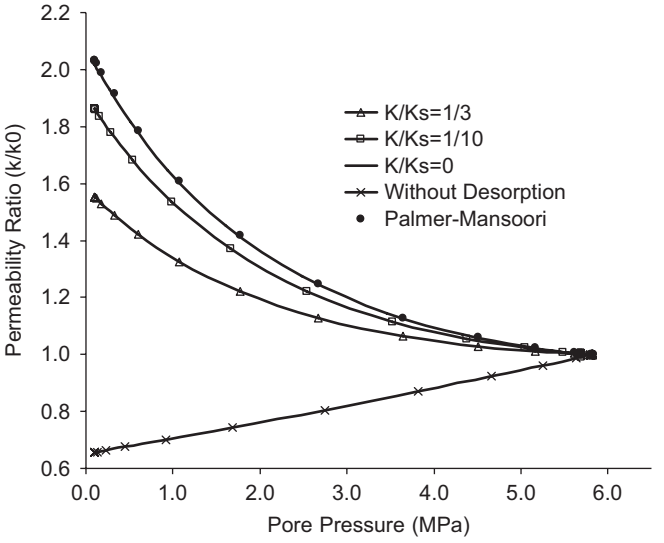

Fig. 5. Example I: impacts of different bulk modulus ratio (K/K_s) and gas desorption on permeability ratio (k/k_0).

4.1.3. Permeability evolution

The spatial and temporal variations of the permeability ratios are shown in Fig. 4. As the pore pressure declines, the permeability ratio increases with time. The permeability in the area near the right edge changes more rapidly than the area far from this edge because the pressure gradient close to right edge is far greater. The steady state is reached at about 20,000 s (~5 h) when the pressure is equal to 1 atm.

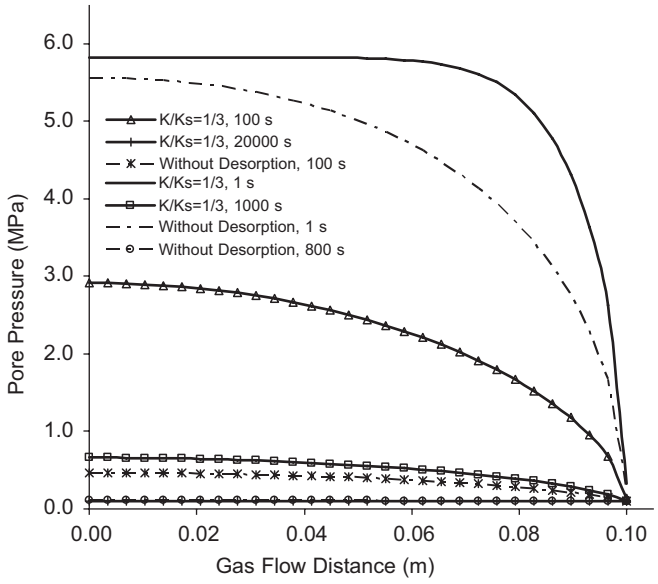

Fig. 6. Example I: spatial and temporal distributions of pore pressure with and without gas desorption ($K/K_s = 1/3$).

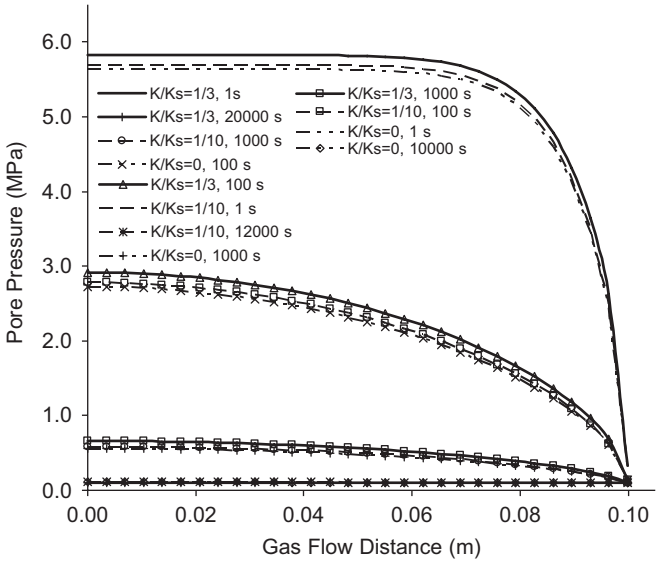

Fig. 7. Example I: impact of different bulk modulus ratio (K/K_s) on the pore pressure distribution.

4.1.4. Impact of modulus ratios on permeability

As shown in Fig. 5, the permeability ratio (k/k_0) increases due to gas desorption when pore pressure decreases. When the ratio of bulk modulus (K/K_s) changes from 1/3 to 0, the highest permeability ratio varies from 1.55 to 2.03. When the bulk modulus of coal grains (K_s) is assumed to be infinite, the simulation result is identical with the data calculated by the Palmer–Mansoori model. If the gas desorption is neglected, the permeability ratio drops linearly to 0.66.

4.1.5. Gas pressure distributions

The spatial and temporal variations of the gas pressure are shown in Figs. 6 and 7. These results demonstrate that gas desorption has a much more significant impact on the gas pressure distribution than the bulk modulus ratios.

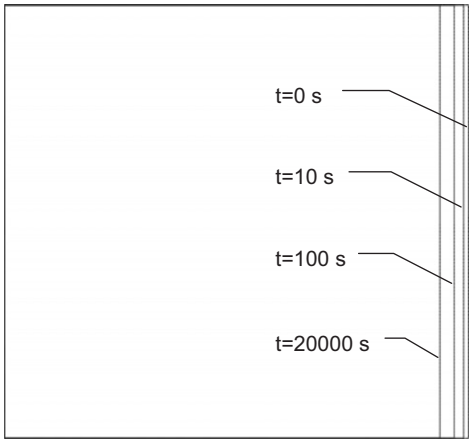

Fig. 8. Example I: evolution of the simulated coal sample configuration with gas desorption.

4.1.6. Coal deformation

As shown in Fig. 8, the coal deformation changes with time due to the gas desorption. It shows that the coal sample shrinks with decreasing pore pressure in the horizontal direction.

The model results presented above reveal the characteristics of the gas desorption from coal as evident in the experiments [7,10]. One of these characteristics is that the gas sorption-induced volumetric strain plays an important role in the variation of coal porosity and permeability. Our model results show that under the conditions of uniaxial strain and constant overburden load, the influence from the coal grain deformation can be neglected when estimating volumetric strain, porosity and pressure evolution. However, the bulk modulus of grains may not be simply treated as infinite when calculating permeability because the cubic relationship between porosity and permeability. A slight change in porosity may result in a much larger change in permeability. If gas desorption is not considered, the permeability may decrease linearly due to the increasing effective stress. Otherwise, gas desorption may increase the permeability and the net change in permeability is controlled by the opposite effects from effective stress and gas desorption. The pore pressure may be underestimated dramatically if the effect of gas desorption is neglected. Although the permeability may decrease without gas desorption and cause gas to flow slowly, the storage coefficient becomes much smaller and pore pressure decreases very quickly. Therefore, the gas absorption capability dominates the storage coefficient.

4.2. Example II: gas desorption under constrained plane strain

The new coupled model is applicable to variable loading conditions. The following example is used to simulate the

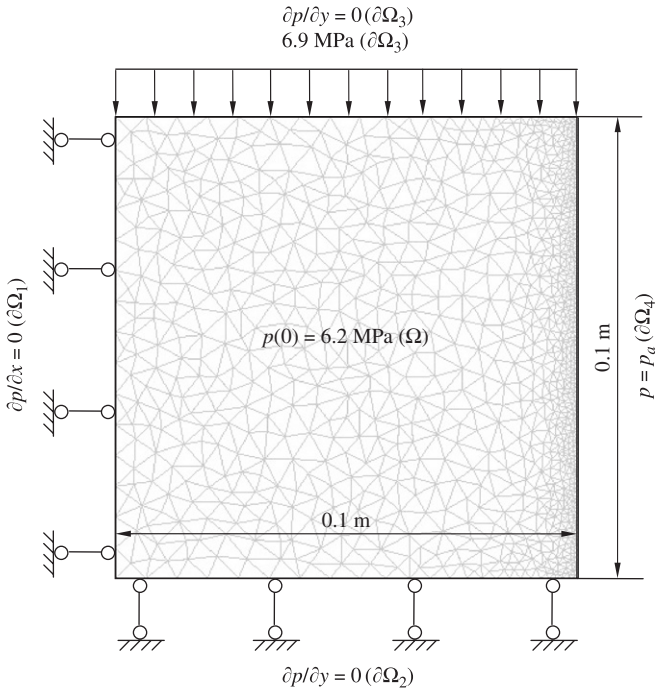

Fig. 9. Example II: simulation model of gas desorption from a coal sample under the plane strain state with a constant overburden load.

coal sample under the constrained plane strain state as shown in Fig. 9.

The same geometrical model and the same material properties (Table 1) are applied as previous. The upper and right sides are unconstrained. The displacements at the left and bottom sides are constrained in the horizontal and vertical directions, respectively. A distributed overburden load of 6.9 MPa is applied on the upper side and remains unchanged during gas desorption. The initial gas pore pressure in the coal is 6.2 MPa and the pressure on the right side remains at 101.325 kPa. Zero fluxes are specified on the other three boundaries.

The relations between gas pressure and permeability ratio under different conditions are shown in Fig. 10. As the pore pressure decreases, the permeability decreases first, then increases after the pressure comes to a critical value of about 1 MPa. The permeability ratio (k/k_0) varies not significantly when the ratio of bulk modulus (K/K_s) changes from 1/3 to 0. The biggest relative difference is 6.7%. However, the maximum permeability ratios calculated by using the Palmer–Mansoori model are significantly higher. The relative error is 141–153%. If the gas desorption is neglected, the permeability ratio decreases to 0.59 linearly. As shown in Fig. 11, the coal shrinks in both directions when the gas pressure declines.

The impact of the different boundary conditions is significant in this example although the property parameters are the same as those in the Example I. The overburden loading and plane strain conditions increase the effective stress and reduce the permeability in contrast to the uniaxially loaded condition in the first example. This difference is the reason why the permeability calculated by

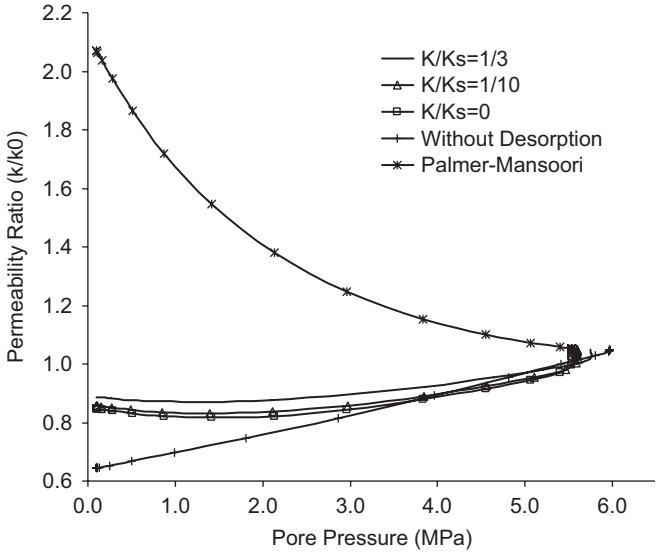

Fig. 10. Example II: impacts of different bulk modulus ratio (K/K_s) and gas desorption on permeability ratio (k/k_0).

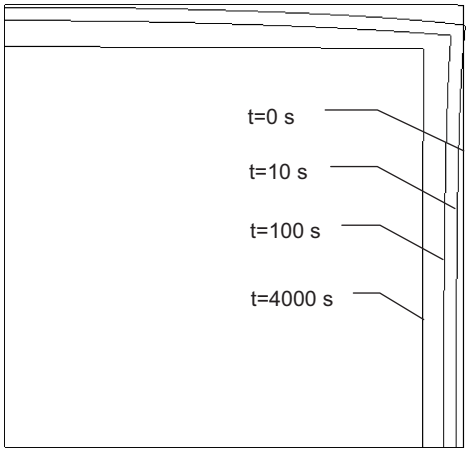

Fig. 11. Example II: evolution of the coal sample configuration with gas desorption.

the Palmer–Mansoori model is much greater than our model results.

4.3. Example III: gas desorption under the unconstrained plane strain

In this example, we change the left boundary of Example I from the constrained horizontal displacement condition to an unconstrained condition, as illustrated in Fig. 12. All other conditions remain the same as Example II.

The relations between gas pressure and permeability ratio under different conditions are shown in Fig. 13. If gas desorption is included, the permeability decreases initially when pore pressure declines. Then it rebounds at the pressure of about 3 MPa and increases to 0.91. The influence of the bulk modulus ratio ($K/K_s = 1/3,\ 1/10,\ 0$) is not significant. If gas desorption is not included, the permeability ratio decreases linearly with decreasing pore

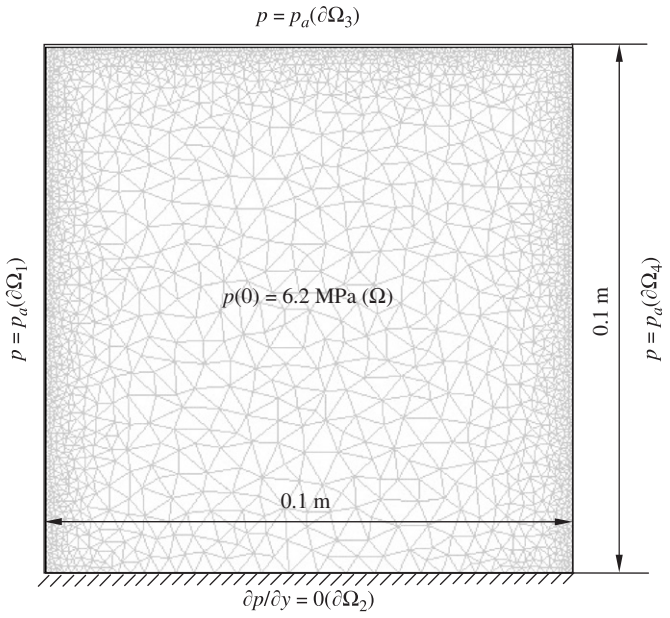

Fig. 12. Example III: simulation model of gas desorption from a coal sample under the unconstrained plane strain state.

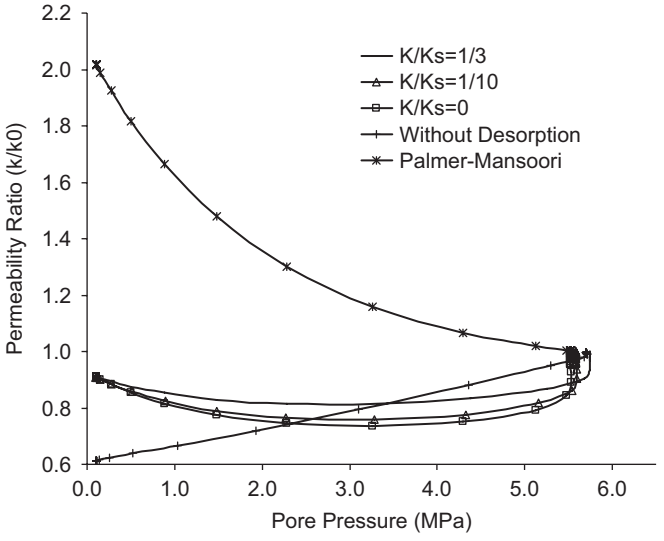

Fig. 13. Example III: impacts of different bulk modulus ratio (K/K_s) and gas desorption on permeability ratio (k/k_0).

pressure. If the Palmer–Mansoori model is applied, the permeability ratio increases throughout and the maximum deviation from the current model is about 121%. As shown in Fig. 14, the coal shrinks both in the horizontal direction and in the vertical direction simultaneously when the gas pressure declines.

This example is analogous to Example II and also demonstrates that the loading and boundary conditions have significant impact on model results. The permeability of our model is much less than that of the Palmer–Mansoori model. The difference indicates that the influence of effective stress is underestimated due to the assumptions in the Palmer–Mansoori model. Only one direction of

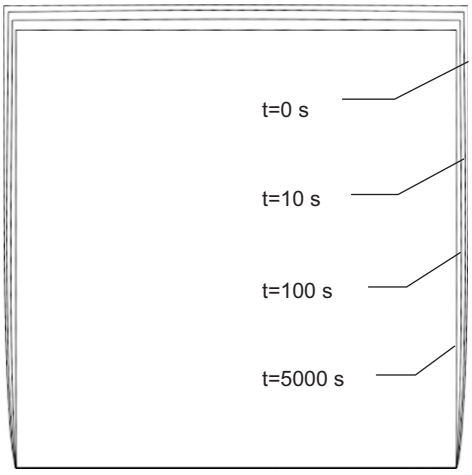

Fig. 14. Example III: evolution of the coal sample configuration with gas desorption.

compressive strain is considered in the Palmer–Mansoori model, so that the impact of gas desorption is exaggerated when neglecting the compressive strain in the other direction.

5. Conclusions

In this study, a new coupled gas flow and sorption-induced coal deformation finite element model is developed to quantify the net change in permeability, the gas flow, and the resultant deformation of the coal seam. The coupling between gas flow and coal deformation is realized through a general porosity and permeability model. The general porosity model considers the principal controlling factors, including the volume occupied by the free-phase gas, the volume occupied by the adsorbed phase gas, the mechanical deformation-induced pore volume change, and the sorption-induced coal pore volume change. More importantly, these factors are quantified under in situ stress conditions. A cubic relation between coal porosity and permeability is introduced to relate the coal storage capability (changing porosity) to the coal transport property (changing permeability). The general porosity and permeability model is then implemented into the new coupled gas flow and coal deformation finite element model.

The FE model has been applied to compare the performance of the new model with that of the Palmer–Mansoori model. It is found that the Palmer–Mansoori model may produce significant errors if loading conditions deviate from the assumptions of the uniaxial strain condition and that of infinite bulk modulus of the coal grain. The FE model has also been applied to conduct a number of simulation examples. The model results have revealed the characteristics of the gas desorption from coal as evident in the experiments reported in the literature. When the pore pressure declines during gas desorption, the net change in permeability accompanying the gas

production is controlled competitively by the effects of declining pore pressure and increasing shrinkage of coal.

Acknowledgment

This work is supported by the Australia Research Council under Grants DP0342446 and DP0209425 and by the Australian Department of Education, Science and Training through the Australia-China Special Fund. This support is gratefully appreciated.

References

[1] Saghafi A, Faiz M, Roberts D. CO_2 storage and gas diffusivity properties of coals from Sydney Basin, Australia. Int J Coal Geol 2007;70:240–54.

[2] Seidle JP, Jeansonne MW, Erickson DJ. Application of matchstick geometry to stress dependent permeability in coals. In: Proceedings of the SPE rocky mountain regional meeting, Casper, Wyoming, 15–21 May 1992, paper SPE 24361.

[3] Gary I. Reservoir engineering in coal seams: Part 1—The physical process of gas storage and movement in coal seams. Soc Petrol Eng Res Eng 1987;1:28–34.

[4] Harpalani S, Chen G. Influence of gas production induced volumetric strain on permeability of coal. Geotech Geol Eng 1997;15:303–25.

[5] Clarkson CR, Bustin RM. The effect of pore structure and gas pressure upon the transport properties of coal: a laboratory and modeling study. 1. Isotherms and pore volume distributions. Fuel 1999;78:1333–44.

[6] Faiz M, Saghafi A, Sherwood N, Wang I. The influence of petrological properties and burial history on coal seam methane reservoir characterisation, Sydney Basin, Australia. Int J Coal Geol 2007;70:193–208.

[7] Harpalani S, Schraufnagel A. Measurement of parameters impacting methane recovery from coal seams. Int J Min Geol Eng 1990;8: 369–84.

[8] Seidle JP, Huitt LG. Experimental measurement of coal matrix shrinkage due to gas desorption and implications for cleat permeability increases. In: Proceedings of the international meeting on petroleum engineering, Beijing, 14–17 November 1995, paper SPE 30010.

[9] Cui X, Bustin RM. Volumetric strain associated with methane desorption and its impact on coalbed gas production from deep coal seams. AAPG Bull 2005;89:1181–202.

[10] Robertson EP, Christiansen RL. Modeling permeability in coal using sorption—induced strain data. In: Proceedings of the 2005 SPE annual technical conference and exhibition, Dallas, 9–12 October 2005, paper SPE 97068.

[11] Palmer I, Mansoori J. How permeability depends on stress and pore pressure in coalbeds: a new model. Soc Petrol Eng Res Eng 1998;12: 539–44.

[12] Shi JQ, Durucan S. Drawdown induced changes in permeability of coalbeds: a new interpretation of the reservoir response to primary recovery. Transp Porous Media 2004;56:1–16.

[13] Robertson EP, Christiansen RL. A permeability model for coal and other fractured, sorptive-elastic media. In: Proceedings of the SPE eastern regional meeting, Canton, OH, 11–13 October 2006, paper SPE 104380.

[14] Zhao C, Xu T, Valliappan S. Numerical modeling of mass transport problems in porous media: a review. Comput Struct 1994;53:849–60.

[15] Zhao Y, Jin Z, Sun J. Mathematical model for coupled solid deformation and methane. Appl Math Modell 1994;18:328–33.

[16] Valliappan S, Zhang W. Numerical modeling of methane gas migration in dry coal seams. Int J Numer Anal Methods Geomech 1996;20:571–93.

[17] Bai M, Meng F, Elsworth D, Abousleiman Y, Roegiers JC. Numerical modeling of coupled flow and deformation in fractured rock specimens. Int J Numer Anal Methods Geomech 1999;23: 141–60.

[18] Bai M, Abousleiman Y, Cui L, Zhang J. Dual-porosity poroelastic modeling of generalized plane strain. Int J Rock Mech Min Sci 1999;36:1087–94.

[19] Gilman A, Beckie R. Flow of coal-bed methane to a gallery. Transp Porous Media 2000;41:1–16.

[20] Rutqvist J, Tsang C. A study of caprock hydromechanical changes associated with CO_2-injection into a brine formation. Environ Geol 2002;42:296–305.

[21] Zhao Y, Hu Y, Zhao B, Yang D. Nonlinear coupled mathematical model for solid deformation and gas seepage in fractured media. Transp Porous Media 2004;55:119–36.

[22] Biot MA. General theory of three-dimensional consolidation. J Appl Phys 1941;12:155–64.

[23] Detournay E, Cheng AHD. Fundamentals of poroelasticity. In: Fairhurst C, editor. Comprehensive rock engineering, vol. 2. Oxford: Pergamon; 1993. p. 113–71.